Energy Reports 9 (2023) 2548–2556

Contents lists available at ScienceDirect

Energy Reports

journal homepage: www.elsevier.com/locate/egyr

Research paper

Design optimisation of wind turbine towers with reliability-based calibration of partial safety factors

Shaikha Al-Sanad [a], Jafarali Parol [a], Lin Wang [b,*], Athanasios Kolios [c]

[a] Energy and Building Research Center, Kuwait Institute for Scientific Research, P.O. Box: 24885 SAFAT, 13109, Kuwait
[b] Department of Mechanical, Materials and Manufacturing Engineering, University of Nottingham, Nottingham, NG7 2RD, United Kingdom
[c] Department of Wind Energy, Technical University of Denmark, Roskilde 399 4000, Denmark

ARTICLE INFO

Article history:
Received 1 May 2022
Received in revised form 14 December 2022
Accepted 19 January 2023
Available online 30 January 2023

Keywords:
Wind turbine tower
Design optimisation
Reliability based calibration
Partial safety factors
Finite element analysis

ABSTRACT

Having an optimal design of the wind turbine tower, with a minimum mass (cost) while fulfilling multiple design constraints, plays an important role in ensuring an economic and safe design of the wind turbine. During the design of wind turbine towers, partial safety factors (PSFs) are currently commonly used to account for the uncertainties in the loads and material properties due to its easy implementation. The values of PSFs given in design standard are generic and are not derived for a specific design. For a site-specific design of wind turbine towers, the details of the load parameters, such as the type of distributions and the coefficient of variation, can be obtained through the condition monitoring system. With these information, the PSFs can be calibrated based on the reliability method, meeting the target reliability index and avoiding over or under engineering of wind turbine tower structures. In this work, a parametric finite element analysis model is integrated with a genetic algorithm to develop a structural optimisation model of wind turbine towers. The optimisation framework minimises the tower mass under multiple design constraints. The optimisation model has been applied to a representative 2.0 MW onshore wind turbine tower. PSFs are calibrated on the basis of reliability. The optimal tower design with calibrated PSFs is compared against the design with un-calibrated PSFs. Results indicate that the tower design with calibrated PSFs achieves a mass reduction of 2.9% in comparison to the design with un-calibrated PSFs.

1. Introduction

Wind power has received increasingly attention over the past decade. Many countries, such as China, America and United Kingdom, have made significant investments in developing wind farms. In 2020, 93 GW new installations of wind turbines were achieved, and the global total wind power capacity has grown to 743 GW as the end of 2020 (Council, 2017).

Wind turbine tower, which is generally made of steel, supports the rotor and nacelle. It also constitutes around 14% to 20% of the capital cost of an onshore wind turbine (Stehly et al., 2018). Additionally, the overall performance of the wind turbine can be remarkably influenced by the tower structural properties, such as the tower stiffness and natural frequencies. Hence, it is critical to achieve an optimal structural design of the wind turbine tower, in order to make sure the design of the wind turbine system is safe and economic.

The methods used in the design of wind turbine towers can be roughly categorised into two types, i.e. (1) partial safety factor (PSF) design, where uncertainties in the uncertain variables are considered by PSFs; and (2) reliability based design, where the uncertainties are accounted for through stochastic modelling.

By far, the PSF design is still the mostly used design method for wind turbine towers due to its easy implementation. The PSF design highly depends on the PSFs, of which values are normally given by design standards, e.g. IEC 61400-1 (Commission, 2005). The values of PSFs given in design standard are generic and are not derived for a specific design. For a site-specific design of wind turbine towers, the details of the load parameters, such as the type of distributions and the coefficient of variation, can be obtained through the condition monitoring system. With these information, the PSFs can be calibrated based on the reliability method, meeting the target reliability index and avoiding over or under engineering of wind turbine tower structures.

Several studies have been performed on the reliability-based design optimisation (RBDO) of wind turbine components. Hu et al. (Hu et al., 2016) studied RBDO of a wind turbine blade utilising surrogate models and a wind load uncertainty model. The optimal design obtained through RBDO reduces the probability of failure and minimises the material cost. Li et al. (Hu et al., 2016) developed a RBDO framework for wind turbine drivetrains to assure

* Corresponding author.
E-mail address: lin.wang1@nottingham.ac.uk (L. Wang).

https://doi.org/10.1016/j.egyr.2023.01.090

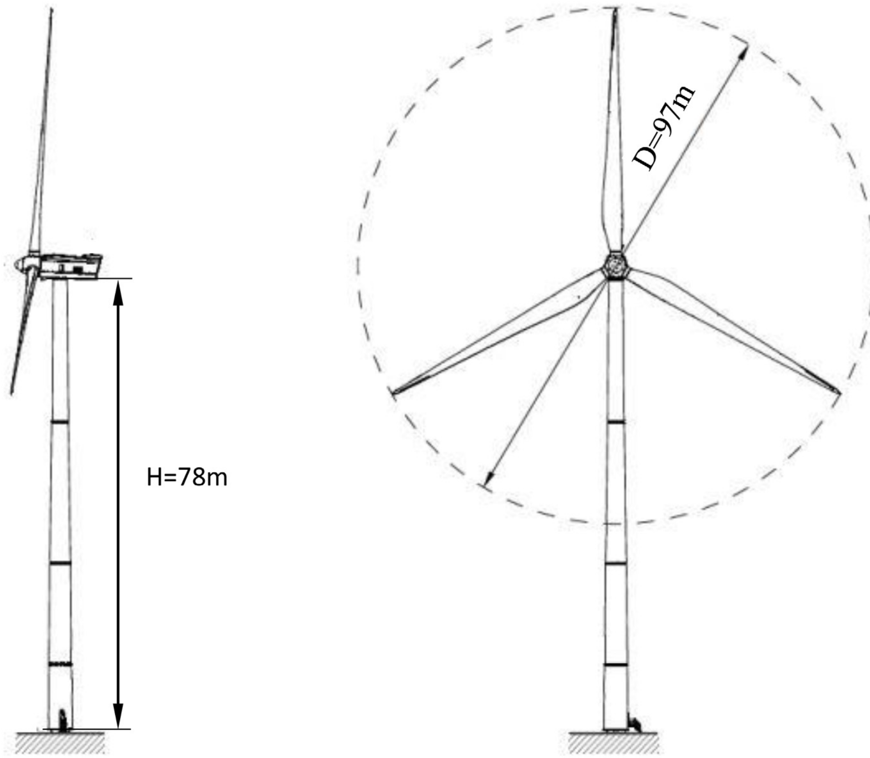

Fig. 1. Layout of a representative 2.0 MW wind turbine.

the target reliability under gear manufacturing and wind load uncertainties. The RBDO framework was applied to a 750 kW wind turbine drivetrain to meet target reliability.

Studies have also been performed on the dynamic response analyses of wind turbine structures considering soil–structure interaction and earthquake. Michel et al. (Michel et al., 2018) performed dynamic analysis of onshore wind turbine foundations considering soil–structure-interaction under seismic loading. Results indicated that the vibration characteristics of the foundations can be affected by the soil properties. Kiyomiya et al. (Kiyomiya et al., 2002) performed dynamic response analysis of onshore wind turbines during earthquakes and wind. Results indicated that the tower has sufficient seismic capacity when the tower is design by wind force under extreme wind speed condition. Soil–structure-interaction and earthquake are not the focus of this paper, and therefore they are not considered in this work.

Finite element analysis has been widely used for modelling wind turbine structures due to it high fidelity (Wang et al., 2016). Genetic algorithm (Mirjalili, 2019), inspired by Darwin's theory of natural evolution, is one of mostly used optimisation algorithm for energy systems and engineering structures (Xu, 2021; Lin and Cheng, 2022). In this work, a design optimisation model for onshore wind turbine towers is established by combining a parametric finite element analysis model and genetic algorithm. PSFs are calibrated on the basis of reliability. The design optimisation model was applied to a typical 2.0 MW onshore wind turbine, optimising its tower structure. The PSFs are calibrated on the basis of reliability. The wind turbine tower is optimised with both calibrated and un-calibrated PSFs.

This paper is arranged into seven sections. Section 2 illustrates the reference wind turbine model. The wind conditions and design loads are presented in Section 3. Section 4 presents the optimisation framework of wind turbine towers. The reliability-based calibration of PSFs is illustrated in Section 5. Section 6 presents results and discussion, while Section 7 presents the conclusions.

Table 1
Specification of a typical 2.0MW wind turbine.

Parameters	Value	Unit
Rated power production	2.0	MW
Rotor diameter	97	m
Number of blades	3	[–]
Rated rotor speed	19	rpm
Tower height	78	m
Tower bottom thickness	0.032	m
Tower top thickness	0.023	m
Tower bottom diameter	4.5	m
Tower top diameter	2.332	m
Rotor and nacelle assembly (RNA) mass	114,000	kg

2. Reference model – 2.0 MW wind turbine

In this work, a representative onshore wind turbine with a rated power of 2MW is taken as a case study. The tower was designed with five different heights, i.e. 78 m, 90 m, 100 m, 104 m and 120 m. In this study, the height of the wind turbine is assumed to be 78 m. The layout of the wind turbine with a 78m-height tower is depicted in Fig. 1, and its specification are presented in Table 1.

3. Wind conditions and loads

3.1. Wind conditions

The wind turbine chosen in this work is deployed in an onshore wind farm, of which location is in Middle East. The distribution of the wind speed measured at the site in 2017 is illustrated in Fig. 2. From Fig. 2 we can observe that the average annual wind speed is about 8.5 m/s. In accordance to IEC 61400-1 (Commission, 2005), this falls in the category of II wind class and the associated extreme wind speed in 50-year return period is 59.5 m/s.

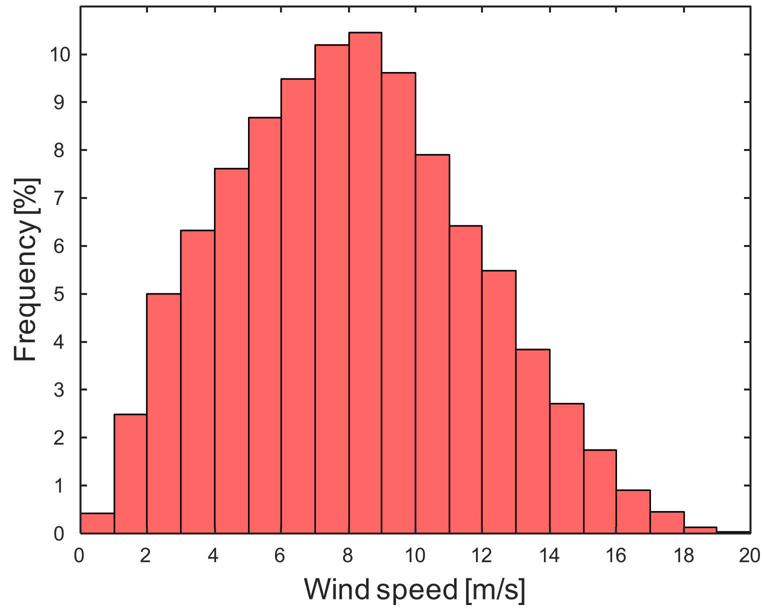

Fig. 2. Distribution of wind speed measured at the site in 2017.

3.2. Loads

The loads on the wind turbine tower are mainly induced from three sources, i.e. (1) gravity loads; (2) aerodynamic loads transferred from rotor blades; (3) wind-induced pressure on the tower itself.

3.2.1. Gravity loads

The RNA weight at the tower top and the weight of the tower contribute to the gravity loads, which can cause the compression on the tower. Therefore, they need to be taken into account when designing wind turbine towers.

3.2.2. Aerodynamic loads transferred from rotor blades

The rotor aerodynamic loads, such as wind thrust and bending moments, are transferable to the tower top. For instance, the rotor thrust force T can be computed by:

$$T = \frac{1}{2}\rho V^2 C_T \pi R^2 \tag{1}$$

where ρ and V are the air density and wind speed, respectively; C_T is the thrust coefficient; R is the radius of the rotor.

3.2.3. Wind-induced pressure on the tower itself

When the wind passes the wind turbine tower, it will induce pressure on the tower. The wind-induced pressure P can be expressed as:

$$P = \frac{1}{2}\rho V(z)^2 C_d \tag{2}$$

where $V(z)$ is the wind velocity at height z; C_d is the drag coefficient, and its value is 0.7 for circular cross sections as suggested in Ref. Commission (2005).

Due to the wind shear, the wind velocity varies with the height. $V(z)$ in Eq. (2) is calculated by:

$$V(z) = V_{hub}\left(\frac{z}{z_{hub}}\right)^{\alpha} \tag{3}$$

where V_{hub} is the wind velocity at the hub centre height; z_{hub} is the hub centre; α is the wind shear parameter, having a common value of 0.2.

Table 2
Ultimate aerodynamic loads.

Items	Value	Unit
$F_{x,u}$	529	kN
$M_{y,u}$	5,251	kN-m

Table 3
Fatigue aerodynamic loads.

Item	Values	Unit
$F_{x,f}$	79	kN
$M_{y,f}$	782	kN-m

3.3. Design load cases (DLCs)

In the design standard IEC 61400-1 (Commission, 2005), 22 DLCs are defined for the design of wind turbines, which covers all potential working conditions of an wind turbine, e.g. start up, normal operation, emergency stop, normal stop, extreme wind condition, etc. These DLCs can be roughly classified into two types, i.e. ultimate and fatigue DLCs. For simplicity, the ultimate load under extreme wind condition in 50-year return period and the fatigue load under normal operation are the typical DCLs utilised in the design of wind turbine structures.

In this work, both ultimate and fatigue DLCs are considered. The ultimate and fatigue loads supplied by the tower manufacturer, which uses NREL FAST code (Jonkman and Buhl, 2005) for load calculations, are listed in Tables 2 and 3. The Damage Equivalent Load (DEL) approach, of which details can be obtained from Ref. Freebury and Musial (2000), was employed to obtain the fatigue loads in Table 3. It is worth mentioning that (1) the loads listed in both Tables 2 and 3 are unfactored values without applying the PSFs; and (2) the subscript u and f in these two tables denotes ultimate and fatigue loads, respectively.

4. Design optimisation model of wind turbine towers

4.1. Parametric FEA model

A parametric FEA model of onshore wind turbine towers is developed utilising ANSYS, a well-known finite element software.

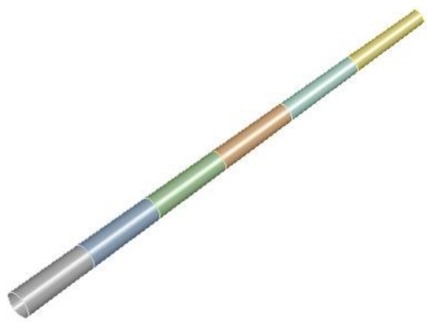

Fig. 3. Geometric model of the tower.

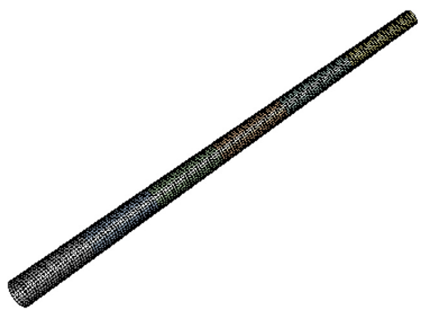

Fig. 4. Structure mesh of the tower.

The geometry, materials, mesh, loads and boundary conditions in the parametric FEA model are illustrated below through the application of the FEA model to the 2.0MW wind turbine tower.

4.1.1. Geometry

Based on the dimensional values presented in Table 1 of Section 2, a geometric model of the 2.0MW wind turbine tower is created. Fig. 3 presents the generated geometric model of the tower.

4.1.2. Materials

The wind turbine tower is made of S355, a low-carbon structural steel commonly utilised for wind turbine support structures. This material is assumed to have isotropic elastic behaviour, with Poisson's ratio of 0.3, Young's modulus of 210 GPa and yield strength of 355 MPa. It should be noted that the tower thickness data do not include the bolts, flanges and paints. In order to account for these, the density of S355 is enlarged from 7850 kg/m^3 to 8500 kg/m^3.

4.1.3. Mesh

A structured mesh method is utilised for creating the mesh of the wind turbine tower. The shell element Shell281 (ANSYS, 2015), a widely used shell element with 8 nodes and 6 degrees of freedom, is utilised. The element size in this study is chosen as 0.5 m, which is determined through a mesh independent study. Fig. 4 depicts the generated structure mesh of the tower.

4.1.4. Loads and boundary conditions

The tower top coordinate system is adopted when applying the loads. A point mass is added on the tower top with rigid connection to account for the RNA mass. The wind thrust force and bending moments, which are the aerodynamic loads transferred from the rotor blades, are applied to the tower top as static loads. The wind-induced pressure is applied to the outer surface of the tower for the ultimate load case. Furthermore, tower bottom is fixed to constrain its movements in all directions.

4.1.5. Solving and post-processing

In this step, the governing equations are solved using finite element method. The simulation results are then post-processed utilising the post-processing tools.

4.2. Design objective

In order to achieve a profitable and economic operation of wind turbines, it is important to reduce the materials cost of the wind turbine tower through mass reduction while satisfying design constraints. The objective function F_{obj} in this study is set to the minimisation of the tower mass m_t. This can be expressed as:

$$F_{obj} = min\,(m_t) \tag{4}$$

4.3. Design variables

Fig. 5 depicts the schematic of the tower structure. From Fig. 5, we can observe that the tower structure consists of six segments with a length of 13 m. It is assumed that the tower diameter is linearly increased from the tower top to the tower bottom. In this study, eight design variables are defined, including the tower bottom and top diameters as well as the thickness of each tower segment. The design variables can be expressed as:

$$X = [x_1\ x_2 \cdots x_n]^T\,, \quad n = 8 \tag{5}$$

where x_1 is the tower top diameter; x_2 is the tower bottom diameter; $x_3$tox_8 are the thicknesses of first to sixth tower segment, respectively.

4.4. Design constraints

4.4.1. Maximum tower top rotation constraint

Large deflections may introduce significant uncertainties and affect the overall stability of the wind turbine tower structure, and therefore it should be avoided. When designing the wind turbine tower structure, the maximum tower top rotation θ_{max} needs not to exceed the allowable rotation θ_{allow}. This constraint can be written as:

$$\theta_{max} \le \theta_{allow} \tag{6}$$

The allowable tower top rotation θ_{allow} in this study is 5°, taken from Ref. Nicholson (2011).

4.4.2. Buckling constraint

Wind turbine towers are normally thin-walled structures, which are prone to experience buckling failure. To stay away from the buckling failure, the buckling load multiplier L_m, which is the ratio of the critical load to the applied load, needs to stand above the minimum allowable load multiplier $L_{m,allow}$. This constraint is written as:

$$L_m \ge L_{m,allow} \tag{7}$$

The allowable load multiplier $L_{m,allow}$ in this work is taken as 1.4 (DNV, 2016).

4.4.3. Fatigue constraint

Wind turbine towers experience remarkable cyclic loads. Every rotor rotation during the operation of a wind turbine causes the variations of the stress in the tower structure. Whether the rotor is rotating or not can be indicated by the availability of the wind turbine. With the rated rotor speed n_{rated} and the availability η_a (98.5%) on the site, the design life number of cycles N_{life} can be

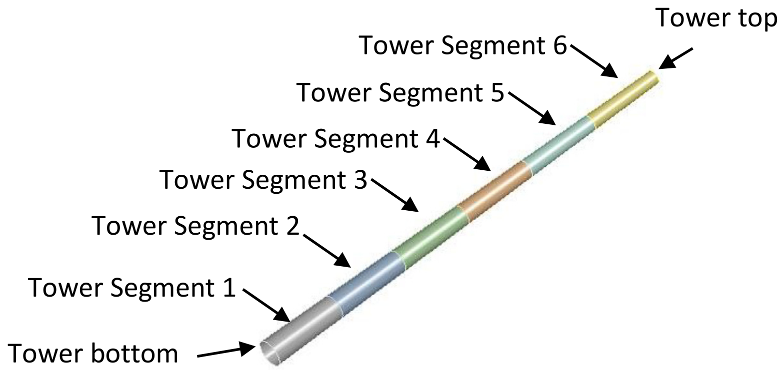

Fig. 5. Schematic of tower structure.

then computed. For a wind turbine tower with a service life time of 20 years, N_{life} can be expressed as:

$$N_{life} = \eta_a \times n_{rated} \times (20\,[\text{year}] \times 365[\text{day/year}] \times 24[\text{hour/day}] \times 60[\text{min/hour}]) \quad (8)$$

With the DEL approach employed in this study, the computational cost is lowered to an equivalent load case, in which the number of cycles to failure N_{DEL} is derived through an equivalent S–N curve. In this study, the S–N curve with an intercept A of 13.93 and a slope m of 4 is taken, as suggested by Ref. Lanier (2005). The design fatigue stress range of $\sigma_{f,design}$ can be obtained using the S–N curve and the design life number of cycles N_{life}, which is computed using Eq. (8). The maximum fatigue stress range $\sigma_{f,max}$ within the tower structure can be calculated using the FEA simulations. The minimum fatigue safety ratio $f_{sr,min}$, which is the ratio of the design fatigue stress range $\sigma_{f,design}$ to the maximum fatigue stress range $\sigma_{f,max}$, should stand above the allowable fatigue safety ratio $f_{sr,allow}$. This constraint can be expressed as:

$$f_{sr,min} \geq f_{sr,allow} \quad (9)$$

The allowable fatigue safety ratio is equal to one times the materials safety factor for fatigue strength $\gamma_{m,f}$. According to IEC 61400-1 (Commission, 2005), the material safety factor fatigue strength needs not be less than 1.1. $\gamma_{m,f}$ in this study is taken as 1.1, and therefore $f_{sr,allow}$ is equal to 1.1.

4.4.4. Ultimate strength constraint

The von-Mises stress σ should stay below the allowable stress σ_{allow}, in order to ensure the structural integrity of the tower under ultimate limit state. This constraint is written as:

$$\sigma \leq \sigma_{allow} \quad (10)$$

The allowable stress σ_{allow} is given by:

$$\sigma_{allow} = \sigma_y/\gamma_m \quad (11)$$

where σ_y is the yield strength, γ_m is the material safety factor.

4.4.5. Vibration constraint

To avoid the occurrence of resonance-induced vibration, the first natural frequency of the wind turbine tower, f_{1st}, should be adequately separated from the f_{1P} and f_{3P}, which are the rotating rotor induced frequency and blade-passing frequency, respectively. The soft–stiff structural design is normally used for wind turbine towers. In this design, the first natural frequency of the wind turbine tower sits between the f_{1P} and f_{3P} frequencies. In this study, f_{1st} is designed to avoid both f_{1P} and f_{3P} frequencies with a tolerance of ±5% (Lloyd and Hamburg, 2010). This constraint is written as:

$$f_{1P+5\%} \leq f_{1st} \leq f_{3P-5\%} \quad (12)$$

For the chosen 2.0 MW wind turbine, it has a cut-in and rated rotor speeds of 9rpm and 19rpm, respectively. Thus, the vibration constraint can be rewritten as:

$$0.333\ \text{Hz} \leq f_{1st} \leq 0.429\ \text{Hz} \quad (13)$$

4.4.6. Design variable constraint

To achieve a feasible and realistic wind turbine tower design, each design variable is restricted to vary within a range. This constraint can be expressed as:

$$x_i^L \leq x_i \leq x_i^U i = 1, 2, \ldots, 8 \quad (14)$$

where x_i^L and x_i^U are the lower and upper bound of the design variables x_i.

The tower bottom generally requires a larger diameter than the tower top, as it needs to resist larger resultant loads. In this study, the tower bottom diameter is constrained to be greater than the tower top diameter. This constraint can be expressed as:

$$x_2 - x_1 \geq 0 \quad (15)$$

Moreover, the thickness of the wind turbine tower generally decreases from the tower bottom to the tower top. To ensure this, the following constraint is applied:

$$x_i - x_{i-1} \geq 0 i = 4, 5, \ldots, 8 \quad (16)$$

4.5. GA and parameters setting in GA

GA is a well-known optimisation algorithm inspired by observing the natural selection process. It is capable of dealing with a large amount of design variables and obtaining global optima, and it has been widely used for optimisation of wind turbine structures (Pourrajabian et al., 2021; Lee and Shin, 2021). Therefore, GA is chosen in this study to find optimal solutions. In the GA, a population of individuals (also referred as candidate solutions) evolves toward better solutions. The properties of each individual, such as genotype and chromosomes, can be mutated and altered. The evolution in the GA starts with an initial population, in which individuals are produced randomly. With the help of mutation and crossover operators, new generation can be created. When either the maximum number of iterations have been produced or a satisfactory fitness level has been achieved by the present population, the GA optimisation process terminates.

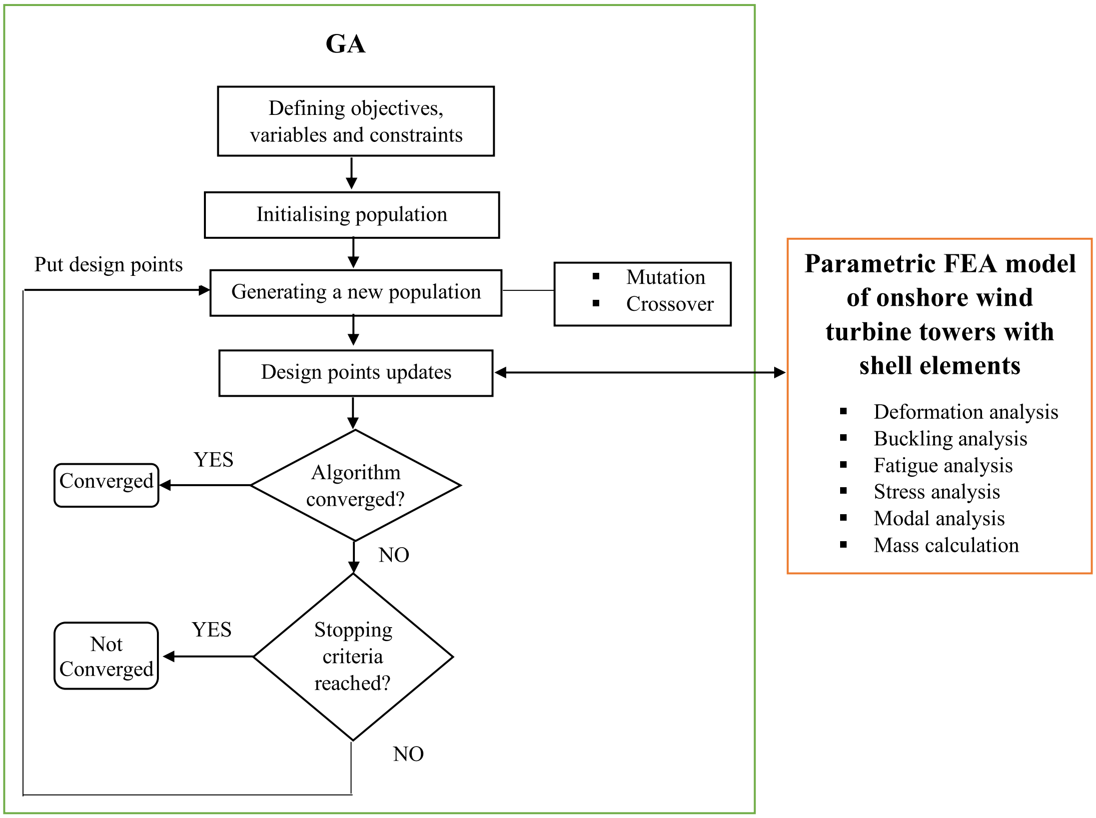

Fig. 6. Flow diagram of optimisation framework for wind turbine towers.

Table 4
Main GA parameters.

Item	Value
Type of initial sampling	Constrained sampling
Number of initial samples N_{Ini}	100
Maximum number of iteration $N_{MaxIter}$	30
Number of samples per iteration $N_{PerIter}$	40
Convergence stability percentage [%]	2
Maximum allowable Pareto percentage [%]	70
Crossover probability	0.82
Mutation probability	0.01

Further information on the GA can be obtained in Ref. Kramer (2017).

Table 4 presents the main parameters of the GA used in this study.

4.6. Flow diagram of the optimisation framework

The flow diagram of the optimisation framework for wind turbine tower, which integrates the parametric FEA model and the GA, is illustrated in Fig. 6.

5. Reliability-based calibration of PSFs

The PSFs utilised in the design of wind turbine towers can be calibrated on a probabilistic basis. The purpose of a reliability-based calibration is to determine a set of calibrated PSFs, ensuring the reliability level obtained by using the calibrated PSFs for design is as close as possible to a specified target reliability level. The implementation of reliability-based calibration is presented below through case studies.

The limit state function can be expressed as:

$$R_d \geq E_d \tag{17}$$

where the subscript d designates design values, E_d is the design load effect, R_d is the resistance.

For an independent input variable x with an arbitrary distribution $F(x)$, the design value x_d is given by (EN, 2002):

$$x_d = F^{-1}\left(\Phi\left(-\alpha\beta\right)\right) \tag{18}$$

where α is the sensitivity factor.

In case of normal distribution, the design value x_d is given by (EN, 2002):

$$x_d = \mu - \alpha\beta\sigma \tag{19}$$

where μ and σ are the mean and standard deviation of the stochastic variable x, respectively.

The target safety level for structural design of wind turbine towers to the normal safety class is generally a probability of failure of 10^{-4}, according to DNV-OS-J101 (DNV, 2014). The typical value of 3.71, which corresponds to 10^{-4} probability of failure, is generally chosen as the target reliability index β_t. The design value x_d meeting the target reliability index is then given by:

$$x_d = \mu - \alpha\beta_t\sigma \tag{20}$$

Having obtained the design values, the associated PSFs can be then obtained by:

$$\boldsymbol{\gamma_m} = \frac{\boldsymbol{x_{m,c}}}{\boldsymbol{x_{m,d}}} \tag{21}$$

$$\boldsymbol{\gamma_f} = \frac{\boldsymbol{x_{f,d}}}{\boldsymbol{x_{f,c}}} \tag{22}$$

where $\boldsymbol{\gamma_m}$ is the material PSFs; $\boldsymbol{x_{m,c}}$ and $\boldsymbol{x_{m,d}}$ are the characteristic and design values of a material property, respectively; $\boldsymbol{\gamma_f}$ is the PSF of a load parameter; $\boldsymbol{x_{f,d}}$ and $\boldsymbol{x_{f,c}}$ are the design and characteristic values of a load parameter, respectively.

Table 5
Stochastic parameters.

Variable	Distribution type	COV
Wind pressure	Normal	0.1
Thrust load	Normal	0.1
Bending moment	Normal	0.1
Yield strength of steel	Lognormal	0.05
Fatigue strength	Lognormal	0.05

6. Results and discussion

6.1. Calibrated PSFs

The reliability-based calibration approach presented in Section 5 is applied to calibrate the PSFs of stochastic parameters involved in the wind turbine tower design. Five stochastic parameters (i.e. wind thrust, wind bending moment, wind pressure, steel yield strength and fatigue strength), which are key parameters and sufficient to describe the structural characteristics of the tower, are chosen in this study for illustration purpose. According to EUROCODE (EN, 2002), lognormal distributions have been usually utilised for material and structural resistance parameters, while normal distributions have been utilised for variable actions for simplicity. Therefore, in this example, the resistance parameters (steel yield strength and fatigue strength) are assumed to have a lognormal distribution, and the variable actions (wind pressure, thrust load and bending moment) are assumed to have a normal distribution. In this work, the COV (coefficient of variation) of steel yield strength and fatigue strength are assumed to be 0.05. The COV of wind pressure, thrust load and bending moment are simply assumed to be 0.1. In practice, the COVs of material properties can be obtained through experimental testing, and the COVs of loads can be measured through load measurement instruments. There is a lack of measured data for the 2MW wind turbine used in this study. Therefore, assumed values of COVs are used in the case study. The stochastic parameters involved in this example are presented in Table 5.

In this example, the PSFs are calibrated to meet the target reliability index of $\beta_t = 3.71$, which corresponds to a probability of failure of 10^{-4}. Table 6 presents the calibrated PSFs. From Table 6 we can observe that the calibrated PSFs are lower than the PSFs given the design standards.

Two examples are presented below to illustrate the details of deriving PSFs.

6.1.1. Example A: Load variable having a normal distribution

In this example, the PSF for a load variable F having a normal distribution is derived. According to EUROCODE (EN, 2002), the characteristic value F_k for a variable action (e.g. wind thrust and bending moment, etc.) is generally taken as its mean μ_F:

$$F_k = \mu_F \tag{23}$$

The design value F_d for a load variable F having normal distribution is given by (EN, 2002):

$$F_d = \mu_F - \alpha_F \beta \sigma_F \tag{24}$$

where subscript F denotes load variable, μ_F and σ_F are the mean and standard deviation of load variable F, respectively; α_F is the sensitivity factor of load variable F, β is the target reliability index.

The coefficient of variation V_F is defined as:

$$V_F = \sigma_F / \mu_F \tag{25}$$

With the help of Eq. (25), Eq. (24) can be rewritten as:

$$F_d = \mu_F \left(1 - \alpha_F \beta V_F\right) \tag{26}$$

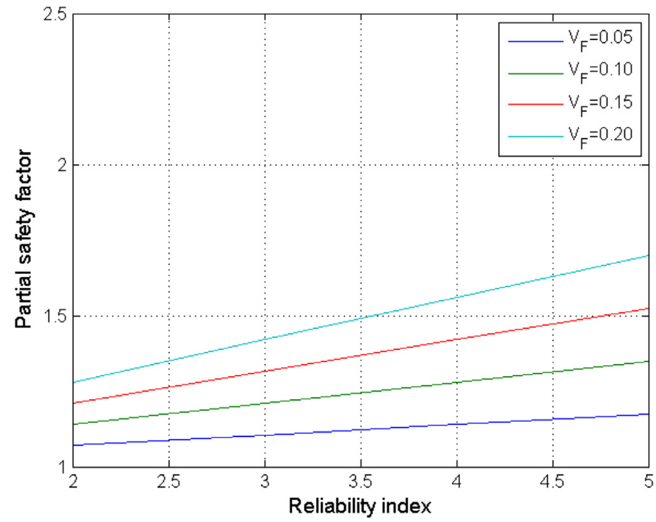

Fig. 7. Variation of γ_F with reliability index β and coefficient of variation V_F. (load variable F having a normal distribution)

The PSF for load variable, γ_F, is given as design value F_d divided by characteristic value F_k, i.e.:

$$\gamma_F = \frac{F_d}{F_k} = \frac{\mu_F \left(1 - \alpha_F \beta V_F\right)}{\mu_F} = 1 - \alpha_F \beta V_F \tag{27}$$

According to ISO 2394 standard (ISO 2014. ISO 2394, 1998), the sensitivity factor α for resistance parameter and load parameter are 0.8 and -0.7, respectively.

Considering the load variable F in this example, the sensitivity factor α is chosen as -0.7. Then Eq. (27) can be rewritten as:

$$\gamma_F = 1 + 0.7 \beta V_F \tag{28}$$

Fig. 7 presents variation of the PSF γ_F with the reliability index β for chosen values of the COV $V_F = 0.05, 0.10, 0.15$ and 0.20. From Fig. 7 we can observe that (1) achieving lower reliability index requires lower PSF; and (2) higher coefficient of variation means higher uncertainties in load and therefore requires higher PSFs to take account of uncertainties.

6.1.2. Example B: Resistance variable having a lognormal distribution

In this example, we aim to derive the PSF for a resistance variable R (strength) having lognormal distribution. The characteristic value R_k and the design value R_d for resistance variable R having lognormal distribution are defined as (Leonardo da Vinci Pilot Project CZ/02/B/F/PP-134007, 2005):

$$R_k = \mu_R \exp\left(-1.645 V_R\right) \tag{29}$$

$$R_d = \mu_R \exp\left(-\alpha_R \beta V_R\right) \tag{30}$$

where subscript R denotes resistance variable.

The PSF for resistance variable, γ_R, is given as characteristic value R_k divided by design value R_d, i.e.:

$$\gamma_R = \frac{R_k}{R_d} = \frac{\exp\left(-1.645 V_R\right)}{\exp(-\alpha_R \beta V_R)} \tag{31}$$

The sensitivity factor for resistance variable R α is chosen as 0.8. Then Eq. (31) can be rewritten as:

$$\gamma_R = \frac{\exp\left(-1.645 V_R\right)}{\exp(-0.8 \beta V_R)} \tag{32}$$

Fig. 8 presents variation of the PSF γ_R with the reliability index β for chosen values of the COV $V_R = 0.05, 0.10, 0.15$ and 0.20.

Table 6
Calibrated PSFs.

Item	PSFs given in IEC Standard (Commission, 2005)	Calibrated PSFs	Note
γ_{f1}	1.35	1.26	PSF for wind pressure under ultimate load case
γ_{f2}	1.35	1.26	PSF for wind thrust load under ultimate load case
γ_{f3}	1.35	1.26	PSF for wind bending load under ultimate load case
γ_{mf}	1.1	1.07	PSF for fatigue strength
γ_{m}	1.1	1.07	PSF for yield strength of steel

Table 7
Comparison of tower design with un-calibrated and calibrated PSFs.

Item	Optimal design with un-calibrated PSFs	Optimal design with calibrated PSFs
Tower top diameter [m]	2.158	2.153
Tower bottom diameter [m]	4.297	4.227
Thickness of first segment [m]	0.0320	0.0319
Thickness of second segment [m]	0.0294	0.0283
Thickness of third segment [m]	0.0261	0.0247
Thickness of fourth segment [m]	0.0227	0.0224
Thickness of fifth segment [m]	0.0200	0.0199
Thickness of sixth segment [m]	0.0169	0.0168
Tower mass [ton]	172	167

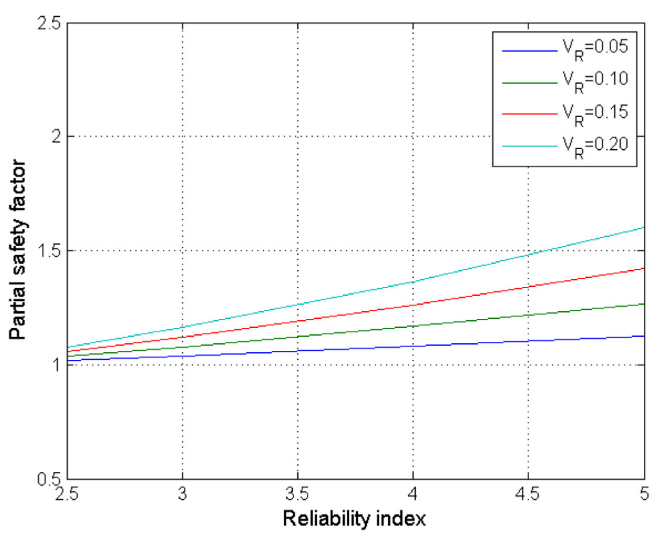

Fig. 8. Variation of PSF γ_R with reliability index β and variation V_R. (resistance variable R having a lognormal distribution).

From Fig. 8 we can observe similar trends as we observed in Example A, i.e. (1) achieving lower reliability index requires lower PSF; and (2) higher coefficient of variation means higher uncertainties in material properties and therefore requires higher PSFs to take account of uncertainties.

6.2. Tower design with un-calibrated and calibrated PSFs

The structural optimisation model presented in Section 4 is used to determine the diameters and thicknesses of the tower. Two design case study with two set of PSFs are considered, i.e. Case (A) design with un-calibrated PSFs; and Case (B) design with calibrated safety factors for a target reliability index of 3.71. The comparison of the design with un-calibrated and calibrated PSFs are presented in Table 7 and Fig. 9. From Table 7 and Fig. 9 we can observe that the design with calibrated PSFs achieves a mass reduction of 2.9% in comparison to the design with un-calibrated PSFs. This indicates that reliability-based calibration of PSFs are useful to optimise the tower structure, meeting target reliability index.

7. Conclusions

In this study, design optimisation of onshore wind turbine towers considering reliability-based calibration safety factors is performed. Through integrating a parametric finite element analysis (FEA) model and a genetic algorithm (GA), a structural optimisation model is developed. The model minimises the tower mass under six design constraints, i.e. maximum tower top rotation, buckling, fatigue, ultimate strength, vibration and design variable constraints. Partial safety factors (PSFs) are calibrated on the basis of reliability. The structural optimisation model was applied to a 2.0 MW onshore wind turbine tower. Design case studies are presented with two set of PSFs, i.e. (1) un-calibrated PSFs; and (2) calibrated PSFs for a target reliability index of 3.71. The conclusions drawn from this work are as follows:

(1) The material and load PSFs can be calibrated to meet the target reliability index;

(2) achieving lower reliability index needs lower PSF;

(3) higher coefficient of variation implies higher uncertainties in load and material parameters and therefore requires higher PSFs to account for uncertainties;

(4) the tower design with calibrated PSFs achieved a 2.9% mass reduction when compared to the design with un-calibrated PSFs, which indicates that reliability-based calibration of PSFs is useful to optimise the tower structure, meeting the target reliability index.

CRediT authorship contribution statement

Shaikha Al-Sanad: Writing – original draft, Investigation, Formal analysis, Methodology. **Jafarali Parol:** Validation, Visualization, Software. **Lin Wang:** Conceptualization, Writing – review & editing. **Athanasios Kolios:** Writing – review & editing, Supervision, Resources.

Declaration of competing interest

The authors declare that they have no known competing financial interests or personal relationships that could have appeared to influence the work reported in this paper.

Data availability

The data that has been used is confidential.

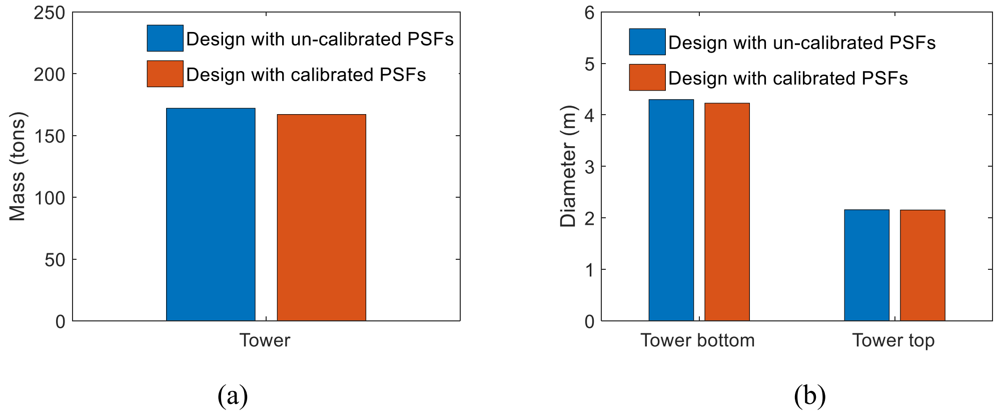

Fig. 9. Comparison of tower design with un-calibrated and calibrated PSFs: (a) tower mass, (b) tower diameter.

References

ANSYS, 2015. ANSYS help documentation. ANSYS, Inc. Theory Release, 8.

Commission, I.E., 2005. IEC 61400-1. Wind turbines–Part, 1.

Council, G.W.E., 2017. GWEC| global wind report 2021.

DNV, 2014. DNV-OS-J101: Offshore standard for design of offshore wind turbine structures.

DNV, G., 2016. DNVGL-ST-0126: Support Structures for Wind Turbines. DNV GL, Oslo, Norway.

EN, B., 2002. BS EN 1990 (2002): Eurocode - basis of structural design.

Freebury, G., Musial, W., 2000. Determining equivalent damage loading for full-scale wind turbine blade fatigue tests. In: 2000 ASME Wind Energy Symposium. p. 50.

Hu, W., Choi, K., Cho, H., 2016. Reliability-based design optimization of wind turbine blades for fatigue life under dynamic wind load uncertainty. Struct. Multidiscip. Optim. 54, 953–970.

ISO 2014. ISO 2394, 1998. General principles on reliability for structures.

Jonkman, J.M., Buhl, M.L., 2005. FAST User's Guide. National Renewable Energy Laboratory Golden, CO, USA.

Kiyomiya, O., Rikiji, T., Van Gelder, P.H., 2002. Dynamic response analysis of onshore wind energy power units during earthquakes and wind. In: The Twelfth International Offshore and Polar Engineering Conference. OnePetro.

Kramer, O., 2017. Genetic algorithms. In: Genetic Algorithm Essentials. Springer.

Lanier, M.W., 2005. LWST Phase I Project Conceptual Design Study: Evaluation of Design and Construction Approaches for Economical Hybrid Steel/Concrete Wind Turbine Towers; June 28, 2002–July 31 2004. National Renewable Energy Lab, Golden, CO (US).

Lee, S.-L, Shin, S.J., 2021. Structural design optimization of a wind turbine blade using the genetic algorithm. Eng. Optim. 1–18.

Leonardo da Vinci Pilot Project CZ/02/B/F/PP-134007, 2005. Implementation of ERUOCODES handbook 2 - reliability backgrounds. https://eurocodes.jrc.ec.europa.eu/publications/handbook-2-reliability-backgrounds. (Accessed on 10 January 2022).

Lin, X., Cheng, M., 2022. Design and application of energy planning scheme based on genetic algorithm. Energy Rep. 8, 393–400.

Lloyd, G., Hamburg, G., 2010. Guideline for the certification of wind turbines. July 1st.

Michel, P., Butenweg, C., Klinkel, S., 2018. Pile-grid foundations of onshore wind turbines considering soil–structure-interaction under seismic loading. Soil Dyn. Earthq. Eng. 109, 299–311.

Mirjalili, S., 2019. Genetic algorithm. In: Evolutionary Algorithms and Neural Networks. Springer.

Nicholson, J.C., 2011. Design of wind turbine tower and foundation systems: optimization approach.

Pourrajabian, A., Dehghan, M., Rahgozar, S., 2021. Genetic algorithms for the design and optimization of horizontal axis wind turbine (HAWT) blades: A continuous approach or a binary one? Sustain. Energy Technol. Assess. 44, 101022.

Stehly, T.J., Beiter, P., Heimiller, D., Scott, G., 2018. 2017 Cost of wind energy review (No. NREL/TP-6A20-72167).

Wang, L., Quant, R., Kolios, A., 2016. Fluid structure interaction modelling of horizontal-axis wind turbine blades based on CFD and FEA. J. Wind Eng. Ind. Aerodyn. 158, 11–25.

Xu, L., 2021. Research on computer interactive optimization design of power system based on genetic algorithm. Energy Rep. 7, 1–13.